FULL PAPER

Dalton
www.rsc.org/dalton

Electrochemical probing of ground state electronic interactions in polynuclear complexes of a new heteroditopic ligand

Edwin C. Constable,*[a] Egbert Figgemeier,*[b] Catherine E. Housecroft,[a] Jerry Olsson[a] and Yves C. Zimmermann[a]

[a] *Department of Chemistry, University of Basel, Spitalstrasse 51, CH-4056 Basel, Switzerland. E-mail: edwin.constable@unibas.ch; Fax: +41 61 2671005; Tel: +41 61 2671001*

[b] *Department of Physical Chemistry, University of Uppsala, P.O. Box 579, 75123 Uppsala, Sweden. E-mail: egbert.figgemeier@fki.uu.se; Fax: +46 18 4713654; Tel: 46 18 4713661*

Received 26th March 2004, Accepted 17th May 2004
First published as an Advance Article on the web 27th May 2004

The synthesis and electronic properties of dinuclear ([(bipy)$_2$Ru(**I**)M(terpy)][PF$_6$]$_4$ (bipy = 2,2′-bipyridine, terpy = 2,2′:6′,2″-terpyridine; M = Ru, Os)) and trinuclear ([{(bipy)$_2$Ru(**I**)}$_2$M][PF$_6$]$_6$ M = Ru, Os, Fe, Co) complexes bridged by 4′-(2,2′-bipyridin-4-yl)-2,2′:6′,2″-terpyridine (**I**) have been investigated and are compared with those of mononuclear model complexes. The electrochemical analysis using cyclic voltammetry and differential pulse voltammetry reveals that there are no interactions in the ground state between adjacent metal centres. However, there is strong electronic communication between the 2,2′-bipyridine and 2,2′:6′,2″-terpyridine components of the bridging ligand. This conclusion is supported by a step-by-step reduction of the dinuclear and trinuclear complexes and the assignment of each electrochemical process to localised ligand sites within the didentate and terdentate domains. The investigation of the electronic absorption and emission spectra reveals an energy transfer in the excited state from the terminating bipy-bound metal centres to the central terpy-bound metal centre. This indicates that the bridge is able to facilitate energy transfer in the excited state between the metal centres despite the lack of interactions in the ground state.

Introduction

Understanding the electronic communication within multinuclear metal complexes is still a challenge despite decades of research. In particular, polypyridine complexes of Ru and Os are currently being investigated and interactions in the excited state have been examined in detail for a number of polypyridine complexes with a range of bridging ligands.[1,2] There is now active interest in the development of integrated chemical systems in which metal complexes play a key role as light-harvesting components, *e.g.* in photoelectrochemical solar cells or models for photosynthetic centres.[3,4] A great number of contributions dealing with intra-molecular energy transfer in the excited state by time resolved laser spectroscopy has been published.[5–32] Interaction parameters in the ground state probed by metal-centred oxidation processes have also attracted significant interest.[2,33,34] On the other hand, there are relatively few electrochemical studies investigating intramolecular interactions of the reduced ground state in multinuclear complexes.[35–38]

Nevertheless, in the light of the application of multinuclear complexes in electroluminescent devices the role of the reduced state of bridging ligands for intramolecular interactions is of great importance.[39] In this context we present here the synthesis, electrochemical properties and fluorescence of di- and trinuclear metal complexes based on 4′-(2,2′-bipyridin-4-yl)-2,2′:6′,2″-terpyridine (**I**) (Scheme 1) as the bridging ligand. Similar bridges have been synthesised and investigated in terms of intra-molecular interactions.[40–44] Whereas these studies focused mainly on investigations of the interactions using absorption spectroscopy and, to a smaller extent, electrochemical techniques, we have focussed our attention on the use of electrochemistry to analyse intra-bridge and inter-metal interactions within the multinuclear complexes. Energy transfer processes within the assemblies in the excited state have been measured and the results are compared with those obtained from the electrochemical investigations.

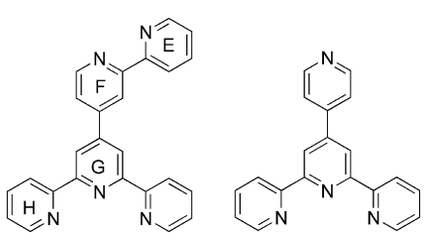

I II

Scheme 1

Experimental

General

Commercially available chemicals were reagent grade and were used without further purification. ^{1}H and ^{13}C NMR spectra were recorded on Bruker AM 250 or 400 and Gemini Varian 300 MHz spectrometers; δ is relative to TMS. IR spectra were recorded on a Mattson Genesis FT spectrophotometer with samples in compressed KBr discs. UV/VIS measurements were performed using a Perkin-Elmer Lambda 19 spectrophotometer and were recorded in MeCN or $CHCl_3$. Fluorescence experiments used a Perkin-Elmer luminescence spectrometer LS 50 and were measured in MeCN or $CHCl_3$. FAB and EI mass spectra were recorded on a VG70–250 or a Finnigan MAT312 instrument. Electrospray mass spectra (ES-MS) were recorded using a Bruker FTMS 4.7T BioAPEX II or a Finnigan MAT LCQ workstation. The microanalyses were performed with a Leco CHN-900. Melting points were measured by a electrothermal digital melting point apparatus. All electrochemical data was measured with a BAS 100 B/W electrochemical workstation and a three-electrode cell, consisting of a silver wire as a pseudo-reference, a glassy carbon disk as the working and a platinum wire as counter electrode, was used. After gaining a full set of voltammograms, ferrocene was added in order to determine the exact position of the signals within the potential window. Tetra-*n*-butylammonium hexafluorophosphate (TBAPF$_6$, 0.1 M) acted as the electrolyte. All solutions were degassed thoroughly for at least 15 min with

DOI: 10.1039/b404602a

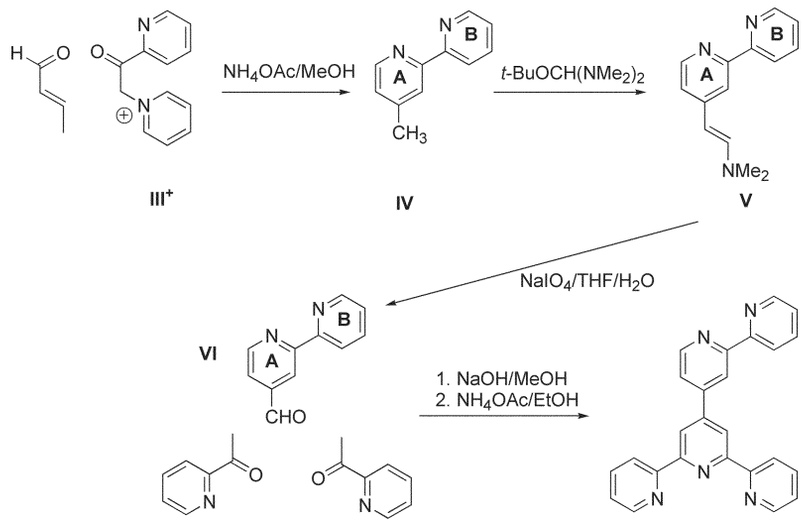

Scheme 2 Reaction scheme for the formation of ligand **I**.

argon and an inert gas blanket was maintained over the solution during the measurements. The preparations of complexes containing ligand **II** are described in a related paper.[45]

4-Methyl-2,2′-bipyridine (IV). A solution of [**III**]$^{+}$I^{-} (Scheme 2) (15 g, 46 mmol), ammonium acetate (15 g, 195 mmol) and crotonaldehyde (3.8 ml, 46 mmol) in MeOH (150 ml) was heated to 65 °C overnight. The solvent was then evaporated *in vacuo* and the black oil extracted with hexane (6 × 50 ml). The combined organic layers were washed with saturated brine and dried over magnesium sulfate. The product was purified by column chromatography (Al_2O_3/hexane–acetone, 9 : 1) followed by recrystallisation *via* shock freezing from light petroleum (bp 40–60 °C) to give **IV** (3.1 g, 40%) as a white powder; mp 62–64 °C; ^{1}H NMR ($CDCl_3$, 250 MHz): δ 8.71 (1H, m, H6B), 8.57 (1H, d, J = 4.8 Hz, H6A), 8.43 (1H, dm, J = 7.8 Hz, H3B), 8.27 (1H, s, H3A), 7.84 (1H, dt, J = 1.7, 7.8 Hz, H4B), 7.33 (1H, m, H5B), 7.17 (1H, m, H5A), 2.47 (3H, s, Me); ^{13}C NMR ($CDCl_3$, 100 MHz): δ 156.6, 156.2, 149.5, 149.3, 148.7, 137.4, 125.1, 124.1, 122.4, 121.7, 21.6; EIMS: *m*/*z* 170 (M^+, 100%); elemental analysis: calc. (%) for $C_{11}H_{10}N_2$: C 77.6, H 5.9, N 16.4; found: C 77.4, H 6.0, N 16.3.

[2-(*N*,*N*-Dimethylamino)vinyl]-2,2′-bipyridine (V). A solution of **IV** (0.282 g, 1.66 mmol) and *tert*-butoxybis(*N*,*N*-dimethylamino)methane (1.0 ml, 4.8 mmol) in dry DMF (5 ml) was degassed with argon for 15 min and then heated to 140 °C under argon for 18 h. The reaction mixture was cooled to room temperature and water (50 ml) was added. The mixture was then extracted with CH_2Cl_2 (5 × 20 ml) and the combined organic layers dried over magnesium sulfate and concentrated *in vacuo*. Purification by column chromatography (Al_2O_3/toluene–diethylamine, 40 : 1) gave **V** (0.350 g, 94%) as a yellow oil. ^{1}H NMR ($CDCl_3$, 400 MHz): δ 8.66 (1H, m, H3A), 8.42 (1H, d, J = 7.8 Hz, H6A), 8.34 (1H, d, J = 5.3 Hz, H6B), 8.13 (1H, d, J = 2.0 Hz, H3B), 7.80 (1H, dt, J = 2.0, 7.6 Hz, H4B), 7.28 (1H, ddd, J 1.2, 5.3, 7.6 Hz, H5B), 7.24 (1H, d, J 13.5 Hz, NCH=), 6.99 (1H, dd, J = 2.0, 7.8 Hz, H5A), 5.11 (1H, d, J = 13.5 Hz, =CHpy), 2.91 (6H, s, NMe_2). ^{13}C NMR ($CDCl_3$, 100 MHz): δ 156.9, 155.5, 149.6, 149.3, 148.9, 144.1, 137.3, 123.8, 121.7, 118.5, 115.2, 94.9, 41.0 (2C); EIMS: *m*/*z* 225 (M^+, 100%); elemental analysis: calc. (%) for $C_{14}H_{15}N_3$: C 74.6, H 6.8, N 18.6; found: C 74.3, H 6.9, N 18.8.

4-Formyl-2,2′-bipyridine (VI). $NaIO_4$ (1.2 g, 5.6 mmol) was added to a solution of **V** (0.338 g, 1.50 mmol) in THF (50 ml) and water (50 ml) The yellow solution was stirred at room temperature for 4 h after which the insoluble products were removed by filtration and washed with tetrahydrofuran. The solvent was evaporated *in vacuo* and CH_2Cl_2 (50 ml) was added. The organic layer was washed with saturated aqueous $NaHCO_3$ (3 × 20 ml), dried over magnesium sulfate and concentrated *in vacuo* to give **VI** (0.226 g, 82%) as a cream coloured solid; mp 85–86 °C (lit. 84.8–86 °C[47]); ^{1}H NMR ($CDCl_3$, 400 MHz): δ 10.19 (1H, s, CHO), 8.90 (1H, d, J = 4.7 Hz, H6A), 8.84 (1H, s, H3A), 8.72 (1H, dm, J = 4.7 Hz, H6B), 8.45 (1H, d, J = 7.3 Hz, H3B), 7.86 (1H, dt, J = 1.7, 7.3 Hz, H4B), 7.73 (1H, dm, J = 4.7 Hz, H5A), 7.37 (1H, dd, J = 1.8, 4.7 Hz, H5B); ^{13}C NMR ($CDCl_3$, 100 MHz): δ 192.0, 175.2, 150.9, 149.2, 143.2, 139.6, 138.2, 125.0, 122.0, 121.9, 121.3. IR: ν(CO) 1704s cm^{-1}; EIMS: *m*/*z* 184 (M^+, 100%); elemental analysis: calc. (%) for $C_{11}H_8N_2O$: C 71.7, H 4.4, N 15.2, O 8.7; found: C 71.9, H 4.7, N 14.8, O 8.6.

4′-(2,2′-Bipyridin-4-yl)-2,2′:6′,2″-terpyridine (I). A solution of 4-formyl-2,2′-bipyridine (0.250 g, 1.36 mmol) and NaOH (1.0 g, 25 mmol) in MeOH (50 ml) was stirred for 5 min at room temperature. 2-Acetylpyridine (0.430 ml, 3.00 mmol) was added and the mixture was stirred for 1 h. Water (100 ml) was added and the mixture was then extracted with CH_2Cl_2 (3 × 50 ml). The organic layers were dried over $MgSO_4$ and concentrated *in vacuo*. The solid residue and ammonium acetate (3.0 g, 39 mmol) in EtOH (100 ml) were heated to reflux overnight. The solution was then cooled, reduced in volume, and water (100 ml) was added. The mixture was extracted with CH_2Cl_2 (3 × 50 ml), and the organic layers were dried over $MgSO_4$ and concentrated *in vacuo*. Purification by column chromatography (Al_2O_3/toluene–diethylamine, 95:5) gave 4′-(2,2′-bipyridin-4-yl)-2,2′:6′,2″-terpyridine (0.286 g, 55%) as an off-white solid. ^{1}H NMR (250 MHz, $CDCl_3$, see Scheme 1 for ring labelling): δ 8.93 (1H, d, J 2.0 Hz, F^3), 8.88 (2 H, s, G^3), 8.84 (1H, dd, J 2.0, 5.0 Hz, F^6), 8.75 (3H, m, H^6, E^6), 8.70 (2 H, d, J 7.7 Hz, H^3), 8.49 (1H, d, J 7.7 Hz, E^3), 7.91 (2H, dt, J 1.7, 7.7 Hz, H^4), 7.88 (1H, m, E^4), 7.83 (1H, m, F^5), 7.38 (3H, m, H^5, E^5). ^{13}C NMR (75 MHz, $CDCl_3$): δ 156.2, 155.7, 149.9, 149.2, 149.1, 147.9, 147.3, 137.1, 124.1 (2C), 124.0 (2C), 121.9, 121.5 (2C), 121.4, 119.3, 119.1. IR (KBr, cm^{-1}): 3045m, 3002w, 1583s, 1566s, 1536s, 1465s, 1440m, 1402m, 1383s, 1358m, 1268w, 1039m, 784s, 732s, 668m, 626s. EI-MS: *m*/*z* 387 (M^+, 100%). Anal. Calc. for $C_{25}H_{17}N_5$ (387.5): C 77.5, H 4.4, N 18.1; found: C 77.6, H 4.7, N 17.7%; mp 159–160 °C.

[(bipy)$_2$Ru(I)][PF$_6$]$_2$. A solution of **I** (0.030 g, 0.077 mmol) and *cis*-[$RuCl_2$(bipy)$_2$]·2H_2O (0.040 g, 0.77 mmol) in EtOH (25 ml) was heated to reflux for 6 h.[46] The solvent was evaporated *in vacuo* and the residue was purified by column chromatography (SiO_2 eluting with MeCN–saturated aqueous KNO_3–H_2O, 7 : 2 : 2). An excess of NH_4PF_6 was added to the

major red–orange fraction and the solution was reduced in volume. The precipitate was collected by filtration over Celite, dissolved in MeCN, and evaporated to dryness to give $[(bipy)_2Ru(\mathbf{I})][PF_6]_2$ (0.080 g, 95%) as a red–orange powder. ^{1}H NMR (400 MHz, CD_3CN, see Scheme 3 for ring labelling): δ 9.12 (1H, d, J 2.4 Hz, F^3), 9.06 (2H, s, G^3), 8.86 (1H, d, J 7.5 Hz, E^3), 8.72 (2H, d, J 7.5 Hz, H^3), 8.56–8.54 (4H, m, A^3, B^3, C^3, D^3), 8.19 (2H, m, H^4), 8.18 (1H, m, E^4), 8.14–8.11 (4H, m, A^4, B^4, C^4, D^4), 8.10 (1H, m, F^6), 8.06 (1H, m, F^5), 7.85–7.76 (7H, overlapping m, A^6, B^6, C^6, D^6, E^6, H^6), 7.52–7.40 (7H, overlapping m, A^5, B^5, C^5, D^5, E^5, H^5). IR (KBr, cm^{-1}): 3430m, 1617m, 1475w, 1446w, 1423w, 842s, 793w, 765m, 558s. UV/VIS (CH_3CN): λ_{max}/nm (ε/dm^3 mol^{-1} cm^{-1}) 242.7 (59400), 286.7 (82500), 461.0 (14500). Fluorescence (CH_3CN): λ_{max}/nm (λ_{ex}/nm) 627.6 (460). ES-MS: m/z 946.0 ([M − PF_6]$^+$), 400.6 ([M − 2PF_6]$^{2+}$). Anal. Calc. for $C_{45}H_{33}N_9RuP_2F_{12}\cdot 3H_2O$ (1144.8): C 47.2, H 3.4, N 11.0; found: C 47.2, H 3.5, N 11.2%. $E°$/V $vs.$ Fc: (Ru^{2+}/Ru^{3+}) 0.93.

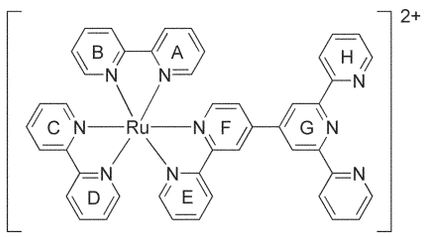

Scheme 3 Ring labelling in $[(bipy)_2Ru(\mathbf{I})]^{2+}$. This labelling is also used in the complexes $[\{(bipy)_2Ru(\mu\text{-}\mathbf{I})\}_2M]^{6+}$ (M = Fe, Ru, Os and Co).

$[(bipy)_2Ru(\mu\text{-}I)Ru(terpy)][PF_6]_4$. A solution of $[(bipy)_2Ru(\mathbf{I})][PF_6]_2$ (0.030 g, 0.027 mmol) and $[Ru(terpy)Cl_3]$[48] (0.012 g, 0.027 mmol) in EtOH (50 ml) with two drops of *N*-ethylmorpholine was heated to reflux for 2 h. The solvent was evaporated *in vacuo* and the residue was purified by column chromatography (silica/acetonitrile–saturated aqueous potassium nitrate–water 7 : 1.5 : 0.5). To the major red–orange fraction an excess of ammonium hexafluorophosphate was added and the solution reduced in volume. The precipitate was collected by filtration through Celite, dissolved in MeCN and evaporated to dryness to afford $[(bipy)_2Ru(\mu\text{-}\mathbf{I})Ru(terpy)][PF_6]_4$ (0.030 g, 64%) as a red–orange powder. ^{1}H NMR (250 MHz, CD_3CN, see Scheme 4 for ring labelling): δ 9.18 (1H, m, F^3), 9.10 (2H, s, G^3), 8.92 (1H, d, J 8.1 Hz, E^3), 8.76 (2H, d, J 8.0 Hz, K^3), 8.67 (2H, d, J 7.9 Hz, H^3), 8.58–8.53 (4H, m, A^3, B^3, C^3, D^3), 8.49 (2H, d, J 8.4 Hz, J^3), 8.44 (1H, t, J 8.0 Hz, K^4), 8.19 (1H, dt, J 2.2, 8.0 Hz, E^4), 8.14–8.04 (6H, m, F^5, F^6, A^4, B^4, C^4, D^4), 7.99–7.88 (4H, m, H^4, J^4), 7.85–7.70 (5H, m, E^6, A^6, B^6, C^6, D^6), 7.53–7.41 (5H, m, E^5, A^5, B^5, C^5, D^5), 7.39–7.33 (4H, m, H^6, J^6), 7.23–7.11 (4H, m, H^5, J^5). IR (KBr, cm^{-1}): 3443m, 3060w, 1605m, 1466m, 1448m, 1421w, 1388m, 1243w, 1029w, 840s, 788m, 765m, 732w, 558s. UV/VIS (CH_3CN): λ_{max}/nm (ε/dm^3 mol^{-1} cm^{-1}) 241.7 (54900), 286.9 (104200), 460.0 (22500), 500.3 (37400). Fluorescence (CH_3CN): λ_{max}/nm (λ_{ex}/nm) 688.8 (460), 691.0 (500). ES-MS: m/z 1570.0 ([M − PF_6]$^+$), 712.5 ([M − 2PF_6]$^{2+}$). Anal. Calc. for $C_{60}H_{44}N_{12}Ru_2P_4F_{24}\cdot 4H_2O$ (1787.1): C 40.3, H 3.0, N 9.4; found: C 40.3, H 3.2, N 9.4%. $E°$/V $vs.$ Fc: (Ru^{2+}/Ru^{3+}) 0.96.

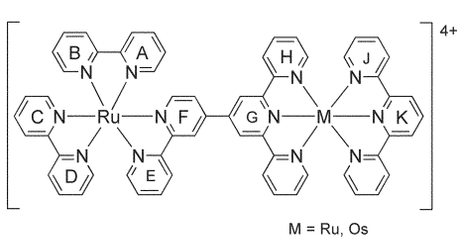

Scheme 4 Ring labelling in $[(bipy)_2Ru(\mu\text{-}\mathbf{I})M(terpy)]^{4+}$ (M = Ru, Os).

$[(bipy)_2Ru(\mu\text{-}I)Os(terpy)][PF_6]_4$. A solution of $[(bipy)_2Ru(\mathbf{I})][PF_6]_2$ (0.010 g, 0.009 mmol) and $[Os(terpy)Cl_3]$[49,50] (0.006 g, 0.027 mmol) in ethylene glycol (4 ml) with two drops of *N*-ethylmorpholine was heated to reflux in a microwave (800 W) for 10 min. A saturated aqueous solution of NH_4PF_6 (25 ml) was added to the brown solution, the precipitate was collected by filtration over Celite and dissolved in MeCN. The solvent was evaporated *in vacuo* and the residue was purified by preparative thin-layer chromatography (SiO_2 eluting with MeCN–saturated aqueous KNO_3–H_2O 7 : 2 : 2). The major brown fraction was dissolved in MeCN, an excess of NH_4PF_6 was added, and the solution was reduced in volume. The precipitate was collected by filtration over Celite, dissolved in MeCN and evaporated to dryness to afford $[(bipy)_2Ru(\mu\text{-}\mathbf{I})Os(terpy)][PF_6]_4$ (0.007 g, 43%) as a dark-brown powder. ^{1}H NMR (400 MHz, CD_3CN, see Scheme 4 for ring labelling): δ 9.26 (1H, m, F^3), 9.17 (2H, s, G^3), 9.04 (1H, d, J 8.0 Hz, E^3), 8.82 (2H, d, J 8.2 Hz, K^3), 8.74 (2H, d, J 8.2 Hz, H^3), 8.63–8.58 (4H, m, A^3, B^3, C^3, D^3), 8.51 (2 H, d, J 8.3 Hz, J^3), 8.23 (1H, dt, J 2.2, 8.0 Hz, E^4), 8.19–8.06 (6H, m, F^5, F^6, A^4, B^4, C^4, D^4), 8.03 (1H, t, J 8.2 Hz, K^4), 7.96 (1H, m, E^6), 7.90–7.78 (8H, m, H^4, J^4, A^6, B^6, C^6, D^6), 7.53–7.48 (5H, m, E^5, A^5, B^5, C^5, D^5), 7.33–7.25 (4H, m, H^6, J^6), 7.21–7.08 (4H, m, H^5, J^5). IR (KBr, cm^{-1}): 3430m, 2924w, 1638w, 1618w, 1466w, 1449m, 1422m, 1384s, 1042w, 836s, 786m, 730w, 558s. UV/VIS (CH_3CN): λ_{max}/nm (ε/dm^3 mol^{-1} cm^{-1}) 286.8 (66900), 310.8 (46300), 497.9 (22600), 669.9 (4000). Fluorescence (CH_3CN): λ_{max}/nm (λ_{ex}/nm) 792.8 (498), 782.1 (671). ES-MS: m/z 1659.0 ([M − PF_6]$^+$), 757.0 ([M − 2PF_6]$^{2+}$). Anal. Calc. for $C_{60}H_{44}N_{12}RuOsP_4F_{24}\cdot 4H_2O$ (1876.2): C 38.4, H 2.8, N 8.9; found: C 38.1, H 2.6, N 8.9%. $E°$/V $vs.$ Fc: (Ru^{2+}/Ru^{3+}) 0.94 (Os^{2+}/Os^{3+}) 0.58.

$[\{(bipy)_2Ru(\mu\text{-}I)\}_2Fe][PF_6]_6$. A solution of $[(bipy)_2Ru(\mathbf{I})][PF_6]_2$ (0.025 g, 0.023 mmol) and $[Fe(H_2O)_6][BF_4]_2$ (0.057 g, 0.017 mmol) in EtOH (50 ml) was heated to reflux for 1 h. The solvent was then evaporated *in vacuo* and the residue purified by column chromatography (SiO_2 eluting with MeCN–saturated aqueous KNO_3–H_2O 7 : 1.5 : 0.5). An excess of NH_4PF_6 was added to the major green–brown fraction and the solution was reduced in volume. The precipitate was collected by filtration through Celite, dissolved in MeCN and evaporated to dryness to yield $[\{(bipy)_2Ru(\mu\text{-}\mathbf{I})\}_2Fe][PF_6]_6$ (0.023 g, 80%) as a red-brown powder. ^{1}H NMR (250 MHz, CD_3CN, see Scheme 4 for ring labelling): δ 9.34 (2H, d, J 2.4 Hz, F^3), 9.32 (4H, s, G^3), 8.98 (2H, d, J 7.9 Hz, E^3), 8.68 (4H, d, J 7.9 Hz, H^3), 8.60–8.54 (8H, m, A^3, B^3, C^3, D^3), 8.24–8.10 (14H, m, F^5, F^6, E^4, A^4, B^4, C^4, D^4), 7.96–7.90 (6H, m, H^4, E^6), 7.86–7.79 (8H, m, A^6, B^6, C^6, D^6), 7.55–7.42 (10H, m, E^5, A^5, B^5, C^5, D^5), 7.18–7.08 (8H, m, H^5, H^6). IR (KBr, cm^{-1}): 3650w, 3450m, 3088w, 2924w, 1720w, 1616m, 1606m, 1533w, 1466m, 1446m, 1423m, 1401m, 1243w, 1027w, 839s, 788m, 762m, 732w, 558s. UV/VIS (CH_3CN): λ_{max}/nm (ε/dm^3 mol^{-1} cm^{-1}) 243.8 (78800), 286.6 (155700), 462.2 (27000), 591.0 (34700). Fluorescence (CH_3CN): λ_{max}/nm (λ_{ex}/nm) 628.0 (460). ES-MS: m/z 1119.1 ([M − 2PF_6]$^{2+}$), 698.8 ([M − 3PF_6]$^{3+}$), 487.1 ([M − 4PF_6]$^{4+}$), 276.4 ([M − 6PF_6]$^{6+}$). Anal. Calc. for $C_{90}H_{66}N_{18}FeRu_2P_6F_{36}\cdot 6H_2O$ (2635.4): C 40.9, H 3.0, N 9.6; found: C 40.3, H 3.3, N 9.4%. $E°$/V $vs.$ Fc: (Ru^{2+}/Ru^{3+}) 0.94, (Fe^{2+}/Fe^{3+}) 0.79.

$[\{(bipy)_2Ru(\mu\text{-}I)\}_2Co][PF_6]_6$. A solution of $[(bipy)_2Ru(\mathbf{I})][PF_6]_2$ (0.016 g, 0.015 mmol) and $[Co(H_2O)_6][BF_4]_2$ (27 mg, 0.0080 mmol) in ethanol (10 ml) was stirred at room temperature for 1 h. The solvent was then evaporated *in vacuo* and the residue was purified by column chromatography (SiO_2 eluting with MeCN–saturated aqueous KNO_3–H_2O 7 : 1.5 : 0.5). An excess of NH_4PF_6 was added to the major orange fraction and the solution reduced in volume. The precipitate was collected by filtration through Celite, dissolved in MeCN and evaporated to dryness to give $[\{(bipy)_2Ru(\mu\text{-}\mathbf{I})\}_2Co][PF_6]_6$ (0.015 g, 81%) as an orange powder. ^{1}H NMR (250 MHz, CD_3CN): δ 91.5 (4H, br, H^6), 52.5 (4H, s, H^3), 36.9 (4H, s, G^3), 32.9 (4 H, s, H^5), 13.9 (2H, s, H_{bipy}), 12.7 (2H, s, H_{bipy}), 10.2 (2H, s, H_{bipy}), 9.8 (4H, s, H^4), 9.2–7.7 (40H, m, H_{bipy}, $A^{3,4,5,6}$, $B^{3,4,5,6}$, $C^{3,4,5,6}$, $D^{3,4,5,6}$). IR

(KBr, cm^{-1}): 3446m, 2924w, 1618m, 1604m, 1561w, 1534w, 1509w, 1467m, 1446m, 1422m, 1384s, 1274w, 1245w, 1028w, 1016w, 839s, 790m, 763m, 731w, 662w, 557s. UV/VIS (CH_3CN): λ_{max}/nm (ε/dm^3 mol^{-1} cm^{-1}) 243.2 (87900), 286.6 (162000), 469.5 (30500). ES-MS: *m*/*z* 1120.1 ($[M - 2PF_6]^{2+}$), 698.4 ($[M - 3PF_6]^{3+}$), 487.6 ($[M - 4PF_6]^{4+}$), 361.3 ($[M - 5PF_6]^{5+}$), 276.7 ($[M - 6PF_6]^{6+}$). Anal. Calc. for $C_{90}H_{66}N_{18}CoRu_2P_6F_{36}\cdot 10H_2O$ (2710.4): C 39.8, H 3.2, N 9.3; found: C 39.8, H 3.5, N 9.4%. $E°$/V *vs.* Fc: (Ru^{2+}/Ru^{3+}) 0.95, (Co^{2+}/Co^{3+}) −0.07.

[{(bipy)$_2$Ru(μ-I)}$_2$Ru][PF$_6$]$_6$. A solution of [(bipy)$_2$Ru(**I**)]-[PF_6]$_2$ (0.010 g, 0.009 mmol) and $RuCl_3\cdot 3H_2O$ (0.001 g, 0.004 mmol) in ethylene glycol (4 ml) together with two drops of *N*-ethylmorpholine was heated to reflux in a microwave oven (800 W) for 6 min. A solution of saturated aqueous NH_4PF_6 (25 ml) was added to the orange solution, and the precipitate was collected by filtration through Celite and dissolved in MeCN. The solvent was evaporated *in vacuo* and the residue was purified by column chromatography (SiO_2 eluting with MeCN–saturated aqueous KNO_3–H_2O 7 : 1.5 : 0.5). An excess of NH_4PF_6 was added to the major red fraction and the solution reduced in volume. The precipitate was collected by filtration through Celite, washed with MeCN and evaporated to dryness to yield [{(bipy)$_2$Ru(μ-**I**)}$_2$Ru][PF_6]$_6$ (0.006 g, 51%) as a red–orange powder. ^{1}H NMR (250 MHz, CD_3CN): δ 9.25 (2H, d, *J* 2.4 Hz, F^3), 9.17 (4H, s, G^3), 8.98 (2H, d, *J* 7.9 Hz, E^3), 8.73 (4H, d, *J* 7.9 Hz, H^3), 8.59–8.54 (8H, m, A^3, B^3, C^3, D^3), 8.23–8.08 (14H, m, F^5, F^6, E^4, A^4, B^4, C^4, D^4), 8.01–7.92 (6H, m, H^4, E^6), 7.86–7.78 (8H, m, A^6, B^6, C^6, D^6), 7.53–7.40 (14H, m, E^5, H^6, A^5, B^5, C^5, D^5), 7.25–7.18 (4H, m, H^5). IR (KBr, cm^{-1}): 3650w, 3443m, 3091w, 2924w, 1617m, 1607m, 1466m, 1447m, 1421m, 1383m, 1244w, 1027w, 837s, 787m, 763m, 731w, 558s. UV/VIS (CH_3CN): λ_{max}/nm (ε/dm^3 mol^{-1} cm^{-1}) 242.4 (51100), 286.4 (118300), 460.0 (17600), 512.1 (38700). Fluorescence (CH_3CN): λ_{max}/nm (λ_{ex}/nm) 670.4 (460), 680.0 (500). ES-MS: *m*/*z* 1141.6 ($[M - 2PF_6]^{2+}$), 713.0 ($[M - 3PF_6]^{3+}$), 498.3 ($[M - 4PF_6]^{4+}$), 369.9 ($[M - 5PF_6]^{5+}$), 283.9 ($[M - 6PF_6]^{6+}$). Anal. Calc. for $C_{90}H_{66}N_{18}Ru_3P_6F_{36}\cdot 6H_2O$ (2680.6): C 40.3, H 2.9, N 9.4; found: C 40.0, H 3.2, N 9.2. $E°$/V *vs.* Fc: (Ru^{2+}/Ru^{3+}) 0.91.

[{(bipy)$_2$Ru(μ-I)}$_2$Os][PF$_6$]$_6$. A solution of [(bipy)$_2$Ru(**I**)]-[PF_6]$_2$ (0.015 g, 0.013 mmol) and $[NH_4]_2[OsCl_6]$ (0.003 g, 0.007 mmol) in ethylene glycol (4 ml) together with two drops of *N*-ethylmorpholine was heated to reflux in a microwave oven (800 W) for 6 min. A solution of saturated aqueous NH_4PF_6 (25 ml) was then added to the dark-brown solution, the precipitate was collected by filtration through Celite and washed with MeCN. The solvent was evaporated *in vacuo* and the residue was purified by column chromatography (SiO_2 eluting with MeCN–saturated aqueous KNO_3–H_2O 7 : 2 : 2). An excess of NH_4PF_6 was added to the major black fraction and the solution reduced in volume. The precipitate was collected by filtration through Celite, washed with MeCN and evaporated to dryness to yield [{(bipy)$_2$Ru(μ-**I**)}$_2$Os][PF_6]$_6$ (0.012 g, 67%) as a dark-brown powder. ^{1}H NMR (250 MHz, CD_3CN): δ 9.25 (2 H, d, *J* 2.4 Hz, F^3), 9.19 (4 H, s, G^3), 9.04 (2 H, d, *J* 8.0 Hz, E^3), 8.74 (4 H, d, *J* 7.9 Hz, H^3), 8.59–8.53 (8 H, m, A^3, B^3, C^3, D^3), 8.23–8.05 (14 H, m, F^5, F^6, E^4, A^4, B^4, C^4, D^4), 7.95–7.89 (14 H, m, H^4, E^6, A^6, B^6, C^6, D^6), 7.55–7.42 (10 H, m, E^5, A^5, B^5, C^5, D^5), 7.29 (4 H, d, *J* 5.2 Hz, H^6), 7.16–7.11 (4 H, m, H^5). IR (KBr, cm^{-1}): 3450m, 2923w, 1617m, 1605m, 1465m, 1445m, 1422m, 1395m, 1353w, 1027w, 837s, 786m, 762m, 730w, 557s. UV/VIS (CH_3CN): λ_{max}/nm (ε/dm^3 mol^{-1} cm^{-1}) 241.3 (53400), 287.1 (112400), 460.0 (21600), 510.3 (37700), 685.7 (8300). Fluorescence (CH_3CN): λ_{max}/nm (λ_{ex}/nm) 767.2 (460), 767.4 (500), 776.6 (690). ES-MS: *m*/*z* 1186.5 ($[M - 2PF_6]^{2+}$), 742.3 ($[M - 3PF_6]^{3+}$). Calc. for $C_{90}H_{66}N_{18}Ru_2OsP_6F_{36}\cdot 4H_2O$ (2733.7): C 39.5, H 2.7, N 9.2; found: C 39.2, H 2.8, N 9.4. $E°$/V *vs.* Fc: (Ru^{2+}/Ru^{3+}) 0.92, (Os^{2+}/Os^{3+}) 0.60.

Results and discussion

Ligand synthesis

The target ligand **I** contains bipy and terpy metal-binding domains directly linked by a C–C bond between the 4- and 4′-positions, respectively. The key synthetic step was to be the generation of an intermediate 1,5-dicarbonyl compound by condensation of 2-acetylpyridine with 2,2′-bipyridine-4-carbaldehyde and subsequent cyclisation to build the central ring of the terpy domain (Scheme 2). The starting bipy derivative **IV** was prepared in reasonable yield by a Kröhnke[47] reaction of the activated pyridinium salt [**III**]I with crotonaldehyde in the presence of ammonium acetate,[51] a method that we find superior in terms of accessibility of starting materials to other published routes.[52–54]

We have found the oxidation of **IV** to the aldehyde **VI** with selenium dioxide[55] gives variable yields; in contrast, our two-step procedure gives excellent and reproducible yields. The reaction of **IV** with Bredereck's reagent $^tBuOCH(NMe_2)_2$[56] gave the *N*,*N*-dimethylaminovinyl derivative **V** in near-quantitative yield. Subsequent oxidation with periodate[57,58] gave **VI** in high yield. The aldehyde is the key intermediate for the preparation of the ditopic ligand **I** containing both the terpy and bipy metal-binding domains. We considered stepwise Kröhnke-type synthesis[47] of **I**, but found that the most reliable method for the preparation of **I** involved the reaction of **VI** with 2-acetylpyridine in the presence of base to give 4-(2,2′-bipyridin-4′-yl)-1,5-bis(2-pyridyl)pentane-1,5-dione. This was not isolated but was reacted *in situ* with ammonium acetate under aerobic conditions to give **I** in 55% isolated yield. The compound was fully characterised by conventional methods. A parent ion was observed at *m*/*z* 387 in the EI mass spectrum. The ^{1}H NMR spectrum was well-resolved with a characteristic singlet assigned to proton 3′ of the terpy domain appearing at δ 8.88.

Preparation and characterisation of complexes

The reaction of ligand **I** with *cis*-[$RuCl_2$(bipy)$_2$]·2H_2O in EtOH at reflux followed by purification and anion exchange, gave [(bipy)$_2$Ru(**I**)][PF_6]$_2$ in 95% yield and in which the bipy domain of **I** is selectively coordinated. The ES-MS of the complex showed major peaks at *m*/*z* 946.0 and 400.6 assigned to $[M - PF_6]^+$ and $[M - 2PF_6]^{2+}$, respectively; isotope patterns matched those calculated. In the ^{1}H NMR spectrum of [(bipy)$_2$Ru(**I**)]-[PF_6]$_2$, a characteristic singlet was observed at δ 8.89, assigned to proton G^3 (see Scheme 2). A COSY experiment allowed the full assignment of the ^{1}H NMR spectrum in which there was significant overlapping of signals arising from corresponding protons on bipy rings A–F.

The preparations of the dinuclear and trinuclear complexes used the 'complexes as ligands' approach.[59] Reaction of [Ru(terpy)Cl_3] with [(bipy)$_2$Ru(**I**)][PF_6]$_2$ in the presence of *N*-ethylmorpholine resulted, after work up, in the isolation of [(bipy)$_2$Ru(μ-**I**)Ru(terpy)][PF_6]$_4$ in 64% yield. The dominant peaks in the ES-MS were at *m*/*z* = 1570.0 and 712.5, consistent with the ions $[M - PF_6]^+$ and $[M - 2PF_6]^{2+}$; isotope patterns were in accord with those simulated for these ions and confirmed the presence of two Ru atoms. The ^{1}H NMR spectrum of [(bipy)$_2$Ru(μ-**I**)Ru(terpy)]$^{4+}$ was assigned by standard COSY techniques. With the exception of new signals assigned to the terminal terpy domain, on going from [(bipy)$_2$Ru(**I**)]$^{2+}$ to [(bipy)$_2$Ru(μ-**I**)Ru(terpy)]$^{4+}$, the ^{1}H NMR spectrum showed only significant changes in chemical shift for protons H^6, H^5 and H^4. The complex [(bipy)$_2$Ru(μ-**I**)Os(terpy)]$^{4+}$ was prepared from [(bipy)$_2$Ru(**I**)]$^{2+}$ and [Os(terpy)Cl_3] under reducing conditions (*N*-ethylmorpholine) in a microwave oven, and was isolated as the $[PF_6]^-$ salt. In the ES-MS, the highest mass peak at *m*/*z* corresponded to $[M - PF_6]^+$. The ^{1}H NMR spectrum of [(bipy)$_2$Ru(μ-**I**)Os(terpy)]$^{4+}$ was assigned by routine methods,

Table 1 Redox potentials of mono-, di- and trinuclear complexes (as PF_6^- salts) in MeCN with [^{n}BuN_4][PF_6] as supporting electrolyte (V, *vs.* internal Fc/Fc^+ reference, error: ± 20 mV)

Complex	Ru^{II}–Ru^{III}	M^{II}–M^{III}	Reductions					Ref.
$[Ru(bipy)_3]^{2+}$	0.88		−1.72	−1.96	−2.17			62
$[Ru(terpy)_2]^{2+}$	0.88		−1.65	−1.90				62
$[Fe(\mathbf{II})_2]^{2+}$		0.80	−1.50	−1.82				63
$[Ru(\mathbf{II})_2]^{2+}$	0.95		−1.54	−1.80				63
$[Os(\mathbf{II})_2]^{2+}$		0.62	−1.47	−1.77				63
$[(bipy)_2Ru(\mathbf{I})]^{2+}$	0.93		−1.61	−1.87	−2.10	−2.57	−2.82	
$[(bipy)_2Ru(\mu\text{-}\mathbf{I})Ru(terpy)]^{4+}$	0.90	0.96	−1.34	−1.68	−1.84	−1.90	−2.23	
$[(bipy)_2Ru(\mu\text{-}\mathbf{I})Os(terpy)_2]^{4+}$	0.94	0.58	−1.37	−1.68	−1.83	−1.92	−2.22	
$[(bipy)_2Ru(\mu\text{-}\mathbf{I})Ru(\mathbf{II})]^{4+}$	0.97	0.97	−1.32	−1.62	−1.78	−1.88	−2.21	
$[(bipy)_2Ru(\mu\text{-}\mathbf{I})Os(\mathbf{II})]^{4+}$	0.94	0.62	−1.37	−1.65	−1.81	−1.93	−2.25	
$[\{(bipy)_2Ru(\mu\text{-}\mathbf{I})\}_2Ru]^{6+}$	0.90	0.98	−1.31	−1.43	−1.73	−1.85	−2.23	
$[\{(bipy)_2Ru(\mu\text{-}\mathbf{I})\}_2Os]^{6+}$	0.91	0.59	−1.33	−1.52	−1.77	−1.89	−2.31	
$[\{(bipy)_2Ru(\mu\text{-}\mathbf{I})\}_2Fe]^{6+}$	0.92	0.78	−1.30	−1.41	−1.73	−1.88	−2.22	
$[\{(bipy)_2Ru(\mu\text{-}\mathbf{I})\}_2Co]^{6+}$	0.95	−0.07	−1.43	−1.60	−1.83	−1.91	−2.27	

and signals for the bridging ligand **I** were at shifts close to those for the same ligand in $[(bipy)_2Ru(\mu\text{-}\mathbf{I})Ru(terpy)]^{4+}$.

The trinuclear complexes $[\{(bipy)_2Ru(\mu\text{-}\mathbf{I})\}_2M]^{6+}$ (M = Fe, Ru, Os and Co) were assembled by reactions of $[(bipy)_2Ru(\mu\text{-}\mathbf{I})]^{2+}$ with $[Fe(H_2O)_6][BF_4]_2$, $RuCl_3{\cdot}3H_2O$ under reducing conditions, $[NH_4]_2[OsCl_6]$ and $[Co(H_2O)_6][BF_4]_2$, respectively. Each was isolated as a $[PF_6]^-$ salt. The ES-MS of each complex gave highest mass peaks corresponding to the parent ion with loss of two $[PF_6]^-$. Observed isotope patterns were in accord with those calculated, giving evidence for the presence of Ru_2Fe, Ru_3, Ru_2Os and Ru_2Co cores, respectively. The ^{1}H NMR spectra of the diamagnetic complexes $[\{(bipy)_2Ru(\mu\text{-}\mathbf{I})\}_2M]^{6+}$ (M = Fe, Ru, Os) were assigned by routine methods. Signals assigned to bridging ligand **I** were at chemical shifts little changed from those in $[(bipy)_2Ru(\mu\text{-}\mathbf{I})M(terpy)]^{4+}$ (M = Ru, Os). In the ^{1}H NMR spectrum of $[\{(bipy)_2Ru(\mu\text{-}\mathbf{I})\}_2Co]^{6+}$, the chemical shifts of the signals assigned to the terminal bipy ligands were, as expected, affected the least by the presence of the paramagnetic Co^{2+} centre. All other protons were significantly paramagnetically shifted. The signals in the terpy domain of ligand **I** could be assigned by comparison with those of $[Co(terpy)_2]^{2+}$ and related complexes for which COSY spectra have been obtained.[60] Although all signals were broadened, only the signal for protons H^6 (the closest to the Co^{2+} centre) was so greatly broadened as to prohibit integration. The relative integrals of the signals at δ 52.5, 36.9, 32.9, 9.8, 13.9, 12.7 and 10.2 were 2 : 2 : 2 : 2 : 1 : 1 : 1 confirming these as belonging to terpy (relative integral 2) or bipy (relative integral 1) domains of the bridging ligand.

Electrochemical characterisation

All of the mono-, di- and trinuclear complexes were electrochemically active in acetonitrile solution. All oxidation and reduction processes observed were quasi-reversible and the potentials for the complexes and for a variety of model substances are presented in Table 1.[61]

Cyclic (A) and differential pulse voltammograms (DPV) (B) for the representative trinuclear complex $[\{(bipy)_2Ru(\mathbf{I})\}_2Fe][PF_6]_6$ are presented in Fig. 1 as examples of the electrochemical response in the oxidative region of all the trinuclear complexes that we have investigated. Two well-defined peaks are observed by both methods and were assigned to the redox-processes of Ru^{II}/Ru^{III} at +0.92 V and Fe^{II}/Fe^{III} at +0.78 V, respectively. The CV indicates quasi-reversible processes while the DPV reveals an expected ratio of the integrated charge for the redox-active species of 2 : 1 within an error of 5%. In the case of the complex $[\{(bipy)_2Ru(\mathbf{I})\}_2Ru][PF_6]_6$, only a single Ru-centred process is observed.

In multinuclear complexes, the electronic interactions between the metal centres are of major importance in determining the physical, photophysical and chemical behaviour of

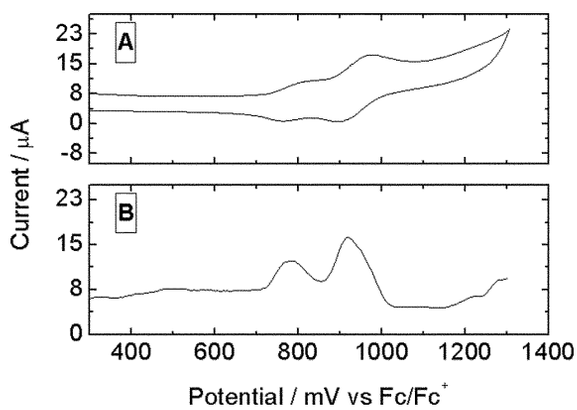

Fig. 1 Cyclic voltammogram (A) and differential pulse voltammogram (B) of the compound $[\{(bipy)_2Ru(\mathbf{I})\}_2Fe][PF_6]_6$ in acetonitrile containing 0.1 M [^{n}BuN_4][PF_6] showing the positive part of the potential window. The potential scale refers to the internal Fc/Fc^+ redox couple, a glassy carbon disk electrode acted as the working electrode and a Pt wire as the counter electrode. The scan rate was 0.1 V s^{-1}.

the compounds.[2] In terms of electrochemistry, the coupling of adjacent metal centres in identical chemical environments results in a peak splitting of the redox-processes, or, more generally, in a shift of the redox potential relative to the mononuclear fragments. The first and most representative example for this behavior is the well known Creutz–Taube ion.[64] In order to investigate the electronic coupling mediated by the bridging ligand **I**, we have studied the electrochemical behavior of $[(bipy)_2Ru(\mu\text{-}\mathbf{I})Ru(terpy)][PF_6]_4$, $[(bipy)_2Ru(\mu\text{-}\mathbf{I})Os(terpy)][PF_6]_4$, $[(bipy)_2Ru(\mu\text{-}\mathbf{I})Ru(\mathbf{II})][PF_6]_4$, $[(bipy)_2Ru(\mu\text{-}\mathbf{I})Os(\mathbf{II})][PF_6]_4$ $[(bipy)_2Ru(\mu\text{-}\mathbf{I})\}_2Fe][PF_6]_6$, $[(bipy)_2Ru(\mu\text{-}\mathbf{I})\}_2Ru][PF_6]_6$, $[(bipy)_2Ru(\mu\text{-}\mathbf{I})\}_2Os][PF_6]_6$ and $[\{(bipy)_2Ru(\mu\text{-}\mathbf{I})\}_2Co]^{6+}$ and redox potentials are listed in Table 1. Table 1 also contains electrochemical data for the parent $[M(bipy)_3]^{2+}$ and $[M(terpy)_2]^{2+}$ complexes together with the potentials of $[M(\mathbf{II})_2][PF_6]_2$ (M = Fe, Ru, Os).[63,65]

A comparison of the Ru^{II}/Ru^{III} redox potential of the complex $[Ru(bipy)_2(\mathbf{I})][PF_6]_2$ with those of the ruthenium-containing trinuclear complexes shows them to be identical within experimental error indicating that there is no electronic coupling mediated by ligand **I**. This conclusion is supported by comparisons of the oxidation waves between other pairs of mononuclear and multinuclear complexes. The electrochemical responses of the central metal ions of $[\{(bipy)_2Ru(\mu\text{-}\mathbf{I})\}_2Fe][PF_6]_6$, $[\{(bipy)_2Ru(\mu\text{-}\mathbf{I})\}_2Ru][PF_6]_6$, $[\{(bipy)_2Ru(\mu\text{-}\mathbf{I})\}_2Os][PF_6]_6$ and $[\{(bipy)_2Ru(\mu\text{-}\mathbf{I})\}_2Fe][PF_6]_6$ are within ±10 mV of those of the mononuclear complexes $[M(\mathbf{II})_2][PF_6]_2$ (M = Fe, Ru, Os).[63,66] Furthermore, the Ru- and Os-centred processes of the complexes $[\{(bipy)_2Ru(\mu\text{-}\mathbf{I})Ru(terpy)][PF_6]_4$, $[(bipy)_2Ru(\mu\text{-}\mathbf{I})Os(terpy)][PF_6]_4$ do not differ from those of the model mononuclear complexes.[67,68]

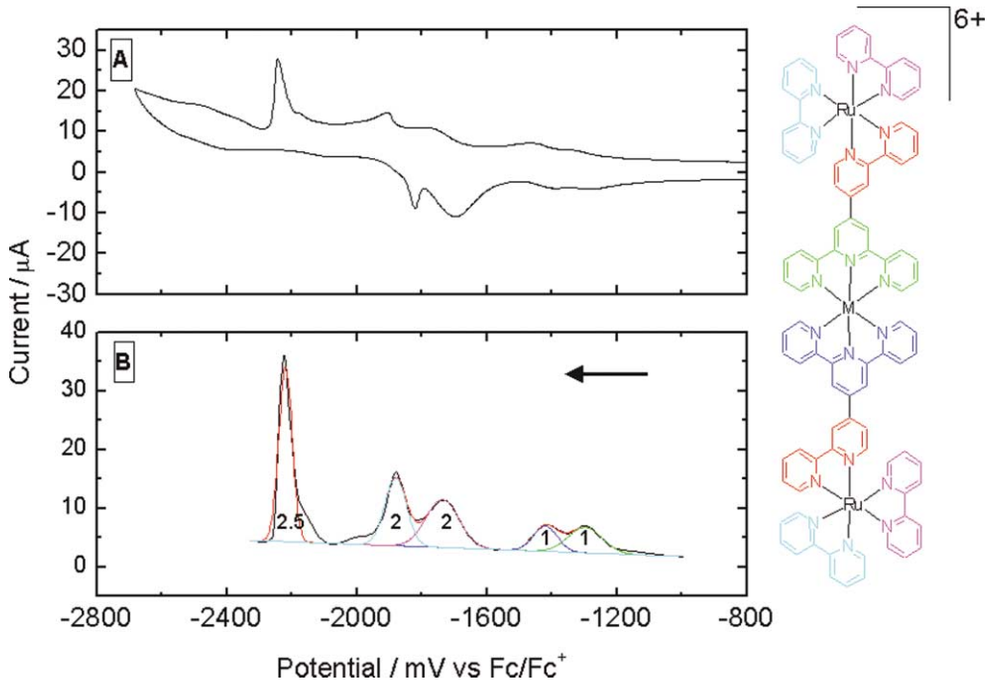

Fig. 2 Cyclic voltammogram (A) and differential pulse voltammogram (B) of the compound $[\{(bipy)_2Ru(\mu\text{-}\mathbf{I})\}_2Fe][PF_6]_6$ in acetonitrile showing the negative part of the potential window. The potential scale refers to the Fc/Fc^+ redox couple, a glassy carbon disk electrode acted as the working electrode and a platinum wire as the counter electrode. The numbers given in (B) indicate the integrated area of the fitted peaks and the arrow indicates the scan direction. The scan rate for the CV was 0.1 V s^{-1}.

Multinuclear complexes that are most similar to those considered in this paper are dinuclear complexes bridged by the 'back-to-back' ligands **VII** and **VIII** (Scheme 5) which are analogues of bipy and terpy, respectively.[40,43] Whereas for $[(bipy)_2Ru(\mu\text{-}\mathbf{VII})Ru(bipy)_2]^{4+}$ a weak electronic interaction is reported,[43] in $[(terpy)Ru(\mu\text{-}\mathbf{VIII})Ru(terpy)]^{4+}$ there is neither splitting of the Ru^{II}/Ru^{III} process nor shifting of the peak with respect to $[Ru(terpy)_2]^{2+}$.[40] Our current results indicate that **I** behaves more like **VIII** than **VII**.

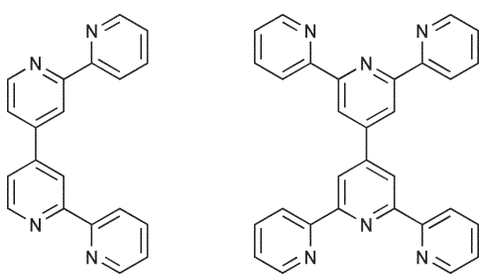

VII VII

Scheme 5

Discussion of ligand reduction

A nearly ideal behavior was observed on the reductive side of the potential window, and this is demonstrated by the plots shown in Fig. 2. The CV is characterised by five quasi-reversible peaks, which also show up in the DPV experiment. The final and sharp peak in the CV at around −2.3 V is irreversible. The shape and the irreversibility is most likely due to a adsorption phenomenon of the highly reduced complexes.[69] Assuming that the LUMOs in the polypyridine complexes are located on the ligands, each reduction can be assigned to specific ligands rather than to a delocalisation on the entire complex.[66] In order to assign these peaks to the ligands, an experiment was performed in which a solution of the monomeric compound $[Ru(bipy)_2(\mathbf{I})]^{2+}$ was doped with drops of an 20 mM acetonitrile solution of $Fe(BF_4)_2$ until the Fe^{2+} concentration reached half of the concentration of $[Ru(bipy)_2(\mathbf{I})]^{2+}$. This titration was monitored by DPV and the result is shown in Fig. 3.

For the starting material, $[Ru(bipy)_2(\mathbf{I})]^{2+}$, five processes were observed (Fig. 3(A)). Three of these peaks are assigned to the step-wise reduction of the three bipyridine ligands, including the bipyridine part of ligand **I**. By a comparison with the electrochemical signature of terpyridine (dashed line, Fig. 3(A)), the peak at lowest potential can be assigned to the terpyridine part of ligand **I**. The signal at −2.30 V could not be assigned to a specific reduction site and is probably caused by the protonation of the non-coordinated terpy part of $[Ru(bipy)_2(\mathbf{I})]^{2+}$. In spite of this uncertainty, the areas of the four dominant peaks are equal within an error of <10% and therefore it can be concluded that each is a product of a one-electron reduction. During the stepwise addition of Fe(II), the peak at most negative potential disappears and two new peaks at −1.30 and −1.40 V evolve (Figs. 3(B) and (C)). At a 2 : 1 ratio of the monomeric complex and Fe(II), the characteristic pattern for the trinuclear complexes could be observed (Fig. 3(D), comparison with the dashed line).

From this experiment, together with the result of the integration of the five peaks in Fig. 2 (1 : 1 : 2 : 2 : 2.5), we can conclude that the two terpyridine ligands of the two bridges in the trinuclear complexes are reduced first. This is also in agreement with the fact that the reduction potentials in $[Ru(terpy)_2]^{2+}$ are less negative than those in $[Ru(bipy)_3]^{2+}$, which implies that in a multinuclear complex with mixed ligands, the terpyridine ligands are reduced before the bipyridine ligands.

The three remaining peaks at most negative potentials (see Fig. 3(B) and (D)) can be assigned to the three different bipyridine domains of the terminal Ru coordination centres. The integration of 2 : 2 : 2 in relation to the first two peaks means that equivalent bipy ligands on both sides of the trinuclear complex are reduced at the same potentials. This indicates that these ligands are not communicating in the reduced state, in contrast to the situation in $[Ru(bipy)_3]^{2+}$.[62] We are left with the problem of assigning the three peaks to the terminal $Ru(bipy)_2$ ligands and to the bipy domain of ligand **I**.

Fig. 4 shows the positions of the reductions of the trinuclear, dinuclear and some model monomeric complexes. The solid lines connect equivalent ligands in related complexes, whereas the red dotted arrows indicate the titration experiment. Moving

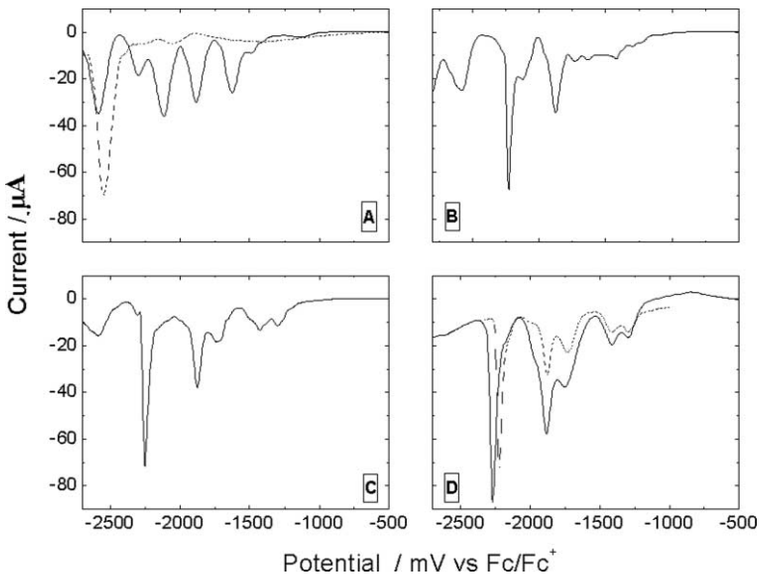

Fig. 3 The titration of $[Ru(bipy)_2(\mathbf{I})]^+$ with $Fe(BF_4)_2$ in MeCN monitored by DPV ((A) = no $Fe(BF_4)_2$ added; (D) = $Fe(BF_4)_2$ concentration is half of $[Ru(bipy)_2(\mathbf{I})]^+$ concentration; (B) and (C) = intermediate concentrations). The scale is standardised to Fc/Fc^+ and the electrode configuration is identical to that described earlier. For comparison, the dashed line in plot A indicates the DPV of terpy in MeCN, and the dashed line in plot D represents the voltammogram of the synthetically isolated $[\{(bipy)_2Ru(\mu\text{-}\mathbf{I})\}_2Fe]$; these were measured separately.

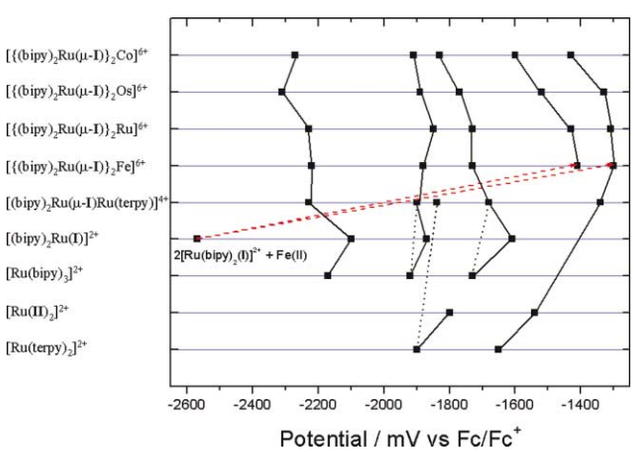

Fig. 4 Correlation of reduction potentials of the trinuclear and dinuclear complexes with model complexes.

from the bottom of the diagram upwards the following picture appears. Modifying a polypyridine ligand by pyridine substituents, *e.g.* $[Ru(terpy)_2]^{2+}$ to $[Ru(\mathbf{II})_2]^{2+}$, results in a shift to less negative potential. The complex $[Ru(bipy)_2(\mathbf{I})]^{2+}$ also follows this trend in relation to $[Ru(bipy)_3]^{2+}$. Assuming that the presence of the terpy substituent in $[Ru(bipy)_2(\mathbf{I})]^{2+}$ affects the bipy domain in **I** more than the other two bipy ligands in the complex, we can conclude that the first reduction of $[Ru(bipy)_2(\mathbf{I})]^{2+}$ is centred on the bipy part of ligand **I**. Coordination of the available terpy ligand in $[Ru(bipy)_2(\mathbf{I})]^{2+}$ with an $\{Ru(terpy)\}^{2+}$ fragment leads to $[(bipy)_2Ru(\mu\text{-}\mathbf{I})Ru(terpy)]^{4+}$, the first reduction of which is at −1.34 V. We assign this peak to a reduction of the bridging terpy domain. The basis of this assignment is a comparison between the potential of the first reduction in the trinuclear complexes, which was defined by the titration experiment described above. The reduction at −1.84 V in $[(bipy)_2Ru(\mu\text{-}\mathbf{I})Ru(terpy)]^{4+}$ is assigned to the terminal terpy ligand by comparison with $[Ru(terpy)_2]^{2+}$ (Fig. 4). The relationship between the three remaining peaks and the bipy ligands in $[(bipy)_2Ru(\mu\text{-}\mathbf{I})Ru(terpy)]^{4+}$ is more difficult to establish. In comparison to $[Ru(bipy)_2(\mathbf{I})]^{2+}$, the three reductions of the bipy ligands in $[(bipy)_2Ru(\mu\text{-}\mathbf{I})Ru(terpy)]^{4+}$ are shifted to more negative potentials. A reasonable explanation for this is that the first reduction of the terpy ligand results in an increase in negative charge density. Assuming that this affects the bipy domain in **I** more than the terminal bipy ligands, one can conclude that the latter are reduced before the bipy unit in ligand **I**. It follows that the peak at −2.23 V in $[(bipy)_2Ru(\mu\text{-}\mathbf{I})Ru(terpy)]^{4+}$ arises from the reduction of the bipy part of bridging ligand **I**. This means that the order of reduction of the bipy domains changes on going from $[Ru(bipy)_2(\mathbf{I})]^{2+}$ to $[(bipy)_2Ru(\mu\text{-}\mathbf{I})Ru(terpy)]^{4+}$.

Following from these results, the following picture emerges for $[\{(bipy)_2Ru(\mu\text{-}\mathbf{I})\}_2Fe]^{6+}$, $[\{(bipy)_2Ru(\mu\text{-}\mathbf{I})\}_2Ru]^{6+}$, $[\{(bipy)_2Ru(\mu\text{-}\mathbf{I})\}_2Os]^{6+}$ and $[\{(bipy)_2Ru(\mu\text{-}\mathbf{I})\}_2Co]^{6+}$. The first two peaks of equal integrated area arise from the reduction of the two terpy ligands. The next two peaks arise from the reduction of the bipy ligands not involved in the bridging ligand. The last reduction is located on the bipy part of bridging ligand **I**. This is illustrated in Fig. 2 in which the different colors code the reduction processes to particular ligand domains. The integral of the last signal in the reductive region was larger than expected. What other process is involved here could not be resolved in detail, but a further reduction of the bridging ligand is likely. This is underlined by the fact that a terpy without any coordination can already be reduced twice.[70]

Although there are no metal–metal interactions in the trinuclear complexes, there is evidence for electronic communication between the 'pillars' of the bridging ligand. In $[\{(bipy)_2Ru(\mu\text{-}\mathbf{I})\}_2Fe]^{6+}$, for example, the reduction of the bipy part of bridging ligand **I** occurs at −2.22 V, *i.e.* a 0.34 V separation from the reductions of the terminal bipy ligands. This is 0.11 V more than the separation between the second and third bipy-based reductions in $[Ru(bipy)_2(\mathbf{I})]^{2+}$. This indicates that the bipy part of ligand **I** in the trinuclear complexes 'feels' the reduction of the terpy domain and therefore the enhanced electron density of the coordinated terpy domain. Assuming a communication between the terpy and the bipy part of the bridging ligand also means that after the reduction of the terpy, part of the additional negative charge can be off-loaded to the bipy. This ability to stabilise the electron after reduction is reflected by the lowered difference between the first and second reductions of the two terpy ligands (ΔE = 0.11 V) of the Fe centre in $[\{(bipy)_2Ru(\mu\text{-}\mathbf{I})\}_2Fe]^{6+}$ compared to the model compound $[Fe(\mathbf{II})_2]^{2+}$ (ΔE = 0.15 V). Moreover, the two first reductions of the multinuclear complexes are taking place at less negative potentials compared with the mononuclear models (see Table 1 and Fig. 4). This suggests a lowering of the LUMO by the coordination of the bridging ligand, whereas the HOMO (represented by the first oxidation) stays in place whether there is a second or third metal coordinated or not. The general

Table 2 Electronic spectroscopic data for the trinuclear and dinuclear complexes and model mononuclear compounds

Complex	λ_{max}/nm (10^{-3} ε/M^{-1} cm^{-1})							Ref.
$[Ru(bipy)_3]^{2+}$		452 (13.0)						62
$[Ru(terpy)_2]^{2+}$		475 (11.6)		307 (52.4)		270 (31.6)		62
$[Fe(\mathbf{II})_2]^{2+}$		569 (24.5)		324 (51.8)	284 (72.0)	276 (64.1)	245 (39.4)	63
$[Ru(\mathbf{II})_2]^{2+}$		488 (30.9)		312 (61.6)		273 (78.4)	238 (43.5)	63
$[Os(\mathbf{II})_2]^{2+}$	668 (7.3)	486 (29.4)		315 (64.4)		275 (71.8)	238 (43.6)	
$[Ru(bipy)_2(\mathbf{I})]^{2+}$			461 (14.5)		287 (82.5)		243 (59.4)	
$[(bipy)_2Ru(\mu\text{-}\mathbf{I})Ru(terpy)]^{4+}$		500 (37.4)			287 (104.2)		242 (54.9)	
$[(bipy)_2Ru(\mu\text{-}\mathbf{I})Os(terpy)]^{4+}$	670 (6)	498 (34)			287 (100)			
$[(bipy)_2Ru(\mu\text{-}\mathbf{I})Ru(\mathbf{II})]^{4+}$		502 (36)	444.0 (17.6) (sh)		285 (89)		242 (45)	
$[(bipy)_2Ru(\mu\text{-}\mathbf{I})Os(\mathbf{II})]^{4+}$	678 (9)	501 (41)	440.0 (18.0) (sh)		285 (114)		235 (67)	
$[\{(bipy)_2Ru(\mu\text{-}\mathbf{I})\}_2Ru]^{6+}$		512 (38.7)	460 (17.6)		286 (118)		242 (51.1)	
$[\{(bipy)_2Ru(\mu\text{-}\mathbf{I})\}_2Os]^{6+}$	686 (8.3)	510 (37.7)	460 (21.6)		287 (112.4)		241 (43.6)	
$[\{(bipy)_2Ru(\mu\text{-}\mathbf{I})\}_2Fe]^{6+}$		591 (34.7)	462 (27.0)		287 (155.7)		244 (78.8)	
$[\{(bipy)_2Ru(\mu\text{-}\mathbf{I})\}_2Co]^{6+}$		470 (30.5)			287 (162.0)		243 (87.9)	

properties described above for $[\{(bipy)_2Ru(\mu\text{-}\mathbf{I})\}_2Fe]^{6+}$ were also observed for $[\{(bipy)_2Ru(\mu\text{-}\mathbf{I})\}_2Ru]^{6+}$ and $[\{(bipy)_2Ru(\mu\text{-}\mathbf{I})\}_2Os]^{6+}$ with respect to the shape and the position of the peaks. For $[\{(bipy)_2Ru(\mu\text{-}\mathbf{I})\}_2Co]^{6+}$, another reduction process was found at −0.93 V which is assigned to the Co(II)/Co(I) reduction. The lower charge density on the Co centre is presumably the reason for the less negative reduction potentials of the ligands in $[\{(bipy)_2Ru(\mu\text{-}\mathbf{I})\}_2Co]^{6+}$ compared to the Fe, Ru and Os-containing trinuclear counterparts (see Table 1).

UV-Vis and fluorescence spectroscopy

The electronic spectra of the model complexes $[Ru(bipy)_3]^{2+}$, $[Ru(terpy)_2]^{2+}$, $[Fe(\mathbf{II})_2][BF_4]_2$, $[Ru(\mathbf{II})_2][BF_4]_2$, $[Os(\mathbf{II})_2][BF_4]_2$, $[Ru(bipy)_2(\mathbf{I})]^{2+}$, $[(bipy)_2Ru(\mu\text{-}\mathbf{I})Ru(terpy)]^{4+}$, $[(bipy)_2Ru(\mu\text{-}\mathbf{I})Os(terpy)]^{4+}$, $[\{(bipy)_2Ru(\mu\text{-}\mathbf{I})\}_2Fe]^{6+}$, $[\{(bipy)_2Ru(\mu\text{-}\mathbf{I})\}_2Ru]^{6+}$, $[\{(bipy)_2Ru(\mu\text{-}\mathbf{I})\}_2Os]^{6+}$ and $[\{(bipy)_2Ru(\mu\text{-}\mathbf{I})\}_2Co]^{6+}$ were measured in MeCN in the range of 200–800 nm. The absorption maxima are listed in Table 2.

The mononuclear complexes are characterised by two spectral regions. Between 200 and 400 nm, a number of peaks and shoulders are present which we assign to ligand-centred π*←π and π* ← n transitions. This region is followed at lower energy by one broad absorption around 500 nm which represents the metal-to-ligand charge transition (MLCT). Both types of transitions are typical of polypyridine complexes.[65] On going from $[Ru(bipy)_2(\mathbf{I})]^{2+}$ to the dinuclear complexes $[(bipy)_2Ru(\mu\text{-}\mathbf{I})Ru(terpy)]^{4+}$ and $[(bipy)_2Ru(\mu\text{-}\mathbf{I})Os(terpy)]^{4+}$, the electronic spectra exhibit an additional shoulder for $[(bipy)_2Ru(\mu\text{-}\mathbf{I})Ru(terpy)]^{4+}$ and a new absorption for $[(bipy)_2Ru(\mu\text{-}\mathbf{I})Os(terpy)]^{4+}$. These observations can be attributed to the additional MLCT taking place on the terpy-coordinated metal centre. The MLCT band for $[Ru(bipy)_2(\mathbf{I})]^{2+}$ is red shifted on going to the dinuclear complexes. This move to lower energy is in qualitative agreement with the findings of the electrochemistry, *i.e.* the lowering of the LUMO in conjunction with an unchanged energy of the HOMO. This assumes that the redox orbitals are equivalent to the spectroscopic orbitals, and that the electrochemical reductions are taking place sequentially on the ligands.[66,71]

In the trinuclear complexes, two distinguishable absorptions are observed in the MLCT region; a representative spectrum is given in Fig. 5. The additional band can be attributed to a second MLCT transition between the central metal (Fe, Ru or Os) and one of the coordinated terpy ligands. With this assumption and by comparison with the mononuclear model complexes, it shows that in the trinuclear complexes the corresponding absorption bands are shifted to lower energies. This observation is also in agreement with the electrochemically observed shift of the first reduction (representing the LUMO) to less negative potentials as discussed above for the dinuclear complexes. An interesting feature is that, in comparison to $[Ru(bipy)_2(\mathbf{I})]^{2+}$, the MLCT transition at 460 nm is not shifted

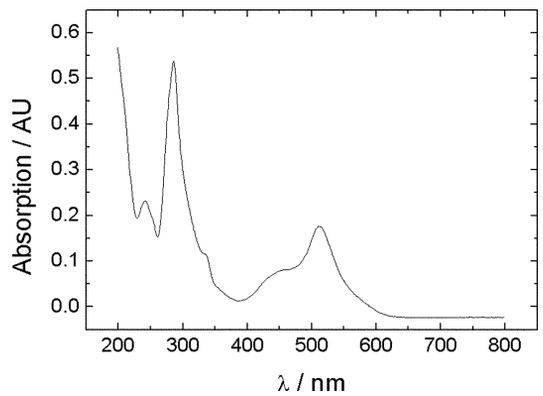

Fig. 5 Absorption spectra of $[\{(bipy)_2Ru(\mu\text{-}\mathbf{I})\}_2Ru][PF_6]_6$ in acetonitrile.

on going to the trinuclear complexes. The electrochemical results were consistent with the metal centred HOMO being unaffected by the complexation of the terpy ligand, and, combined with the electronic spectroscopic data, we can conclude that the lowest lying ligand orbital for the terminating Ru groups is also not shifted due to the addition of metal ions.

The luminescence data (Table 3) were recorded in MeCN and at room temperature. In order to probe the luminescence properties selectively for the different metals involved, the excitation wavelength was varied according to the absorption properties. Exciting $[Ru(bipy)_2(\mathbf{I})]^{2+}$ at 454 nm results in an emission (λ_{em}) at 628 nm, which is reasonably close to that observed for $[Ru(bipy)_3]^{2+}$.[62] On going from $[Ru(bipy)_2(\mathbf{I})]^{2+}$ to $[(bipy)_2Ru(\mu\text{-}\mathbf{I})Ru(terpy)]^{4+}$, one observes a significant red shift of the emission band. Similar values for the emission were also observed for $[(bipy)_2Ru(\mu\text{-}\mathbf{I})Ru(\mathbf{II})]^{4+}$ and $[\{(bipy)_2Ru(\mu\text{-}\mathbf{I})\}_2Ru]^{6+}$. Assuming that the emission takes place from a ^{3}MLCT state, the observed shift of the emission band to lower energy is in agreement with the shift of the electrochemically observed LUMO to less negative potentials.[62]

The mixed metal di- and trinuclear complexes exhibit a somewhat different picture to that of the homometallic ruthenium complexes. When excited at around 500 nm, $[\{(bipy)_2Ru(\mu\text{-}\mathbf{I})\}_2Os]^{6+}$ and $[(bipy)_2Ru(\mu\text{-}\mathbf{I})Os(terpy)]^{4+}$ show luminescence bands only at 767 and 793 nm, respectively. From a comparison with the mononuclear Os complexes and based on the electrochemical data, this points to an Os-centred emission from the ^{3}MLCT state. A surprising feature is that the same emission was detected when $[\{(bipy)_2Ru(\mu\text{-}\mathbf{I})\}_2Os]^{6+}$ and $[(bipy)_2Ru(\mu\text{-}\mathbf{I})Os(terpy)]^{4+}$ were excited at around 450 nm, the wavelength at which both the Ru- and Os-based MLCT transition should occur. This suggests that an efficient energy transfer takes place between the Ru–bipy and the Os–terpy centres, facilitated by the bridging ligand. This feature was observed for all dinuclear and trinuclear complexes involving Os. For the multinuclear, ruthenium-only complexes, only one emission

Table 3 Luminescent data of trinuclear, dinuclear and model mononuclear compounds at different excitation wavelengths (λ_{ex})

Complex	λ_{em}/nm ($\lambda_{ex} \approx 450$ nm (^{1}MLCT))[a]	λ_{em}/nm ($\lambda_{ex} \approx 500$ nm (^{1}MLCT))[a]	Ref.
$[Ru(bipy)_3]^{2+}$	615		62
$[Os(terpy)_2]^{2+}$	615	718	65,74
$[Ru(terpy)_2]^{2+}$	*ca.* 640 (480)		65,74
$[Ru(bipy)_2(\mathbf{I})]^{2+}$	628 (454)		
$[(bipy)_2Ru(\mu\text{-}\mathbf{I})Ru(terpy)]^{4+}$	689 (460)	691 (500)	
$[(bipy)_2Ru(\mu\text{-}\mathbf{I})Os(terpy)]^{4+}$		793 (498)	
$[(bipy)_2Ru(\mu\text{-}\mathbf{I})Ru(\mathbf{II})]^{4+}$		686 (503)	
$[(bipy)_2Ru(\mu\text{-}\mathbf{I})Os(\mathbf{II})]^{4+}$		776 (501)	
$[\{(bipy)_2Ru(\mu\text{-}\mathbf{I})\}_2Ru]^{6+}$	670 (460)	681 (513)	
$[\{(bipy)_2Ru(\mu\text{-}\mathbf{I})\}_2Os]^{6+}$	767 (446)	767 (510)	

[a] Room temperature, acetonitrile solvent.

band was observed, independent of the excitation wavelength. From electrochemical results, the LUMO of $[\{(bipy)_2Ru(\mu\text{-}\mathbf{I})\}_2Ru]^{6+}$ is localised on the $\{Ru(terpy)_2\}$-fragment and it could be suggested that the emission stems also from there, implying an energy transfer from the bipy-coordinated to the terpy-coordinated Ru. Similar results are obtained for $[(bipy)_2Ru(\mu\text{-}\mathbf{I})Ru(terpy)]^{4+}$. This is a somewhat surprising feature, since complexes containing Ru(terpy) units are normally not luminescent at room temperature due to fast deactivation processes involving the ^{3}MC state.[42] Nevertheless, a few examples of Ru(terpy) complexes with long-lived excited state properties have recently been reported.[72,73]

Electronic interactions

The difference between the interactions between the metal centres and between the two sides of the bridging ligand is remarkable and indicates that different orbitals are involved in the two interactions. An interaction between the metal centres is mediated by the overlap of the d(π)-orbitals with the π-acceptor ligand, and by the extension of the π-system of the ligand. In our case, the π-system between the terpy and bipy domains of ligand **I** is obviously interrupted, and this is consistent with the well-established non-planar conformation observed for adjacent phenyl or pyridine rings.[75] Our results also indicate that purely electrostatic interactions do not influence the position of the oxidation of the complexes considered in this paper. On the other hand, in the bridging ligand, a lowering of the LUMO and an efficient distribution of the negative charge seems to take place despite the interruption of the conjugation between the terpy and bipy domains of the bridge. The σ-bond skeleton of the polypyridine ligand and field effects are the mediators of these effects. Altnernatively, it can be speculated that the negative charge on the bridging ligand leads to a planar conformation due to the gain of energy by delocalising the additional charge over an extended conjugated system. This was suggested for related dinuclear complexes the mechanism leading to a strong communication between the metal centres.[39] The shift of λ_{em} from $[Ru(bipy)_2(\mathbf{I})]^{2+}$ to $[(bipy)_2Ru(\mu\text{-}\mathbf{I})Ru(terpy)]^{4+}$ and $[\{(bipy)_2Ru(\mu\text{-}\mathbf{I})\}_2Ru]^{6+}$, respectively, also shows that the excited electron is already delocalised onto the terpy part of the bridging ligand.

Conclusions

We have shown that the metal centres of the di- and trinuclear complexes bridged by the 'back-to-back' terpy-bipy ligand **I** do not interact with each other in the ground state, whereas there is significant communication between the two sides of the bridging ligand upon reduction. Analysis of the absorption and emission spectra indicate that there is energy transfer and, therefore, an interaction between the different coordination sites. This stresses the fact that one has to distinguish clearly between interaction forces in the ground state (probed electrochemically) and in the excited state (probed spectroscopically). In terms of supramolecular chemistry, this means that in the ground state, the metal centres are independent entities and therefore the dinuclear and trinuclear complexes are supramolecular species, whereas in the excited state, there is a strong interaction and energy transfer occurs neglecting the independence of the parts of the entire complex.

Acknowledgements

We thank the Schweizerischer Nationalfonds zur Förderung der wissenschaftlichen Forschung and the University of Basel for the financial support of the work.

References

1 F. Barigelletti and L. Flamigni, *Chem. Soc. Rev.*, 2000, **29**, 1.
2 M. D. Ward, *Chem. Soc. Rev.*, 1995, **24**, 121.
3 C. A. Bignozzi, R. Argazzi and C. J. Kleverlaan, *Chem. Soc. Rev.*, 2000, **29**, 87.
4 L. C. Sun, L. Hammarstrom, B. Akermark and S. Styring, *Chem. Soc. Rev.*, 2001, **30**, 36.
5 V. Balzani, P. Ceroni, A. Juris, M. Venturi, S. Campagna, F. Puntoriero and S. Serroni, *Coord. Chem. Rev.*, 2001, **219**, 545.
6 A. C. Benniston, V. Grosshenny, A. Harriman and R. Ziessel, *Angew. Chem., Int. Ed. Engl.*, 1994, **33**, 1884.
7 C. A. Bignozzi, R. Argazzi, J. R. Schoonover, K. C. Gordon, R. B. Dyer and F. Scandola, *Inorg. Chem.*, 1992, **31**, 5260.
8 C. A. Bignozzi, R. Argazzi, C. Chiorboli, F. Scandola, R. B. Dyer, J. R. Schoonover and T. J. Meyer, *Inorg. Chem.*, 1994, **33**, 1652.
9 C. A. Bignozzi, J. R. Schoonover and F. Scandola, A supramolecular approach to light harvesting and sensitisation of wide-bandgap semiconductors: Antenna effects and charge separation,in *Molecular Level Artificial Photosynthetic Materials*, John Wiley & Sons Inc., New York, 1997, vol. 44, pp. 1–95.
10 A. K. Bilakhiya, B. Tyagi and P. Paul, *Polyhedron*, 2000, **19**, 1233.
11 S. Campagna, S. Serroni, F. Puntoriero, F. Loiseau, L. De Cola, C. L. Kleverlaan, J. Becher, A. P. Sorensen, P. Hascoat and N. Thorup, *Chem.–Eur. J.*, 2002, **8**, 4461.
12 C. Chiorboli, M. A. J. Rodgers and F. Scandola, *J. Am. Chem. Soc.*, 2003, **125**, 483.
13 R. L. Cleary, K. J. Byrom, D. A. Bardwell, J. C. Jeffery, M. D. Ward, G. Calogero, N. Armaroli, L. Flamigni and F. Barigelletti, *Inorg. Chem.*, 1997, **36**, 2601.
14 N. H. Damrauer and J. K. McCusker, *J. Phys. Chem. A*, 1999, **103**, 8440.
15 L. De Cola and P. Belser, *Coord. Chem. Rev.*, 1998, **177**, 301.
16 L. De Cola, V. Balzani, F. Barigelletti, L. Flamigni, P. Belser, A. von Zelewsky, M. Frank and F. Vogtle, *Mol. Cryst. Liq. Cryst. Sci. Technol. Sect. A: Mol. Cryst. Liq. Cryst.*, 1994, **252**, 97.
17 H. Durr and S. Bossmann, *Acc. Chem. Res.*, 2001, **34**, 905.
18 M. Furue, K. Maruyama, Y. Kanematsu, T. Kushida and M. Kamachi, *Coord. Chem. Rev.*, 1994, **132**, 201.
19 M. Furue, M. M. Ishibashi, A. Satoh, T. Oguni, K. Maruyama, K. Sumi and M. Kamachi, *Coord. Chem. Rev.*, 2000, **208**, 103.
20 V. Grosshenny, A. Harriman, M. Hissler and R. Ziessel, *J. Chem. Soc., Faraday Trans.*, 1996, **92**, 2223.
21 M. T. Indelli, F. Scandola, J. P. Collin, J. P. Sauvage and A. Sour, *Inorg. Chem.*, 1996, **35**, 303.
22 O. Johansson, M. Borgstrom, R. Lomoth, M. Palmblad, J. Bergquist, L. Hammarstrom, L. C. Sun and B. Akermark, *Inorg. Chem.*, 2003, **42**, 2908.

23 A. Juris, L. Prodi, A. Harriman, R. Ziessel, M. Hissler, A. El-ghayoury, F. Y. Wu, E. C. Riesgo and R. P. Thummel, *Inorg. Chem.*, 2000, **39**, 3590.
24 A. F. Morales, G. Accorsi, N. Armaroli, F. Barigelletti, S. J. Pope and M. D. Ward, *Inorg. Chem.*, 2002, **41**, 6711.
25 T. Ohno, K. Nozaki, N. Ikeda and M. Haga, *Adv. Chem. Ser.*, 1991, 215.
26 T. Ohno, K. Nozaki and M. Haga, *Inorg. Chem.*, 1992, **31**, 548.
27 E. A. Plummer, J. W. Hofstraat and L. De Cola, *Dalton Trans.*, 2003, 2080.
28 F. Scandola, R. Argazzi, C. A. Bignozzi, C. Chiorboli, M. Indelli and M. A. Rampi, *Coord. Chem. Rev.*, 1993, **125**, 283.
29 F. Scandola, R. Argazzi, C. A. Bignozzi and M. T. Indelli, *J. Photochem. Photobiol. A: Chem.*, 1994, **82**, 191.
30 M. Staffilani, P. Belser, F. Hartl, C. J. Kleverlaan and L. De Cola, *J. Phys. Chem. A*, 2002, **106**, 9242.
31 A. Vlcek, *Coord. Chem. Rev.*, 1998, **177**, 219.
32 M. D. Ward, C. M. White, F. Barigelletti, N. Armaroli, G. Calogero and L. Flamigni, *Coord. Chem. Rev.*, 1998, **171**, 481.
33 S. Fanni, C. Di Pietro, S. Serroni, S. Campagna and J G. Vos, *Inorg. Chem. Commun.*, 2000, **3**, 42.
34 D. M. Guldi, M. Maggini, E. Menna, G. Scorrano, P. Ceroni, M. Marcaccio, F. Paolucci and S. Roffia, *Chem.–Eur. J.*, 2001, **7**, 1597.
35 M. Marcaccio, F. Paolucci, C. Paradisi, M. Carano, S. Roffia, C. Fontanesi, L. J. Yellowlees, S. Serroni, S. Campagna and V. Balzani, *J. Electroanal. Chem.*, 2002, **532**, 99.
36 M. Marcaccio, F. Paolucci, C. Paradisi, S. Roffia, C. Fontanesi, L. J. Yellowlees, S. Serroni, S. Campagna, C. Denti and V. Balzani, *J. Am. Chem. Soc.*, 1999, **121**, 10081.
37 M. Krejcik and A. Vlcek, *Inorg. Chem.*, 1992, **31**, 2390.
38 M. Carano, P. Ceroni, C. Fontanesi, M. Marcaccio, F. Paolucci, C. Paradisi and S. Roffia, *Electrochim. Acta*, 2001, **46**, 3199.
39 S. Welter, K. Brunner, J. W. Hofstraat and L. De Cola, *Nature*, 2003, **421**, 54.
40 E. C. Constable and M. D. Ward, *J. Chem. Soc., Dalton Trans.*, 1990, 1405.
41 J. P. Collin, P. Laine, J. P. Launay, J. P. Sauvage and A. Sour, *J. Chem. Soc., Chem. Commun.*, 1993, 434.
42 L. Hammarstrom, F. Barigelletti, L. Flamigni, M. T. Indelli, N. Armaroli, G. Calogero, M. Guardigli, A. Sour, J. P. Collin and J. P. Sauvage, *J. Phys. Chem. A*, 1997, **101**, 9061.
43 A. J. Downard, G. E. Honey, L. F. Phillips and P. Steel, *Inorg. Chem.*, 1991, **30**, 2259.
44 M. Beley, S. Chodorowskikimmes, J. P. Collin, P. Laine, J. P. Launay and J. P. Sauvage, *Angew. Chem., Int. Ed. Engl.*, 1994, **33**, 1775.
45 E. Figgemeier, E. C. Constable, C. E. Housecroft and Y. C. Zimmermann, 2004, submitted for publication.
46 B. P. Sullivan, D. J. Salmon and T. J. Meyer, *Inorg. Chem.*, 1978, **17**, 3334.
47 F. Kröhnke, *Synthesis*, 1976, 1.
48 E. C. Constable, A. Thompson, D. A. Tocher and M. A. M. Daniels, *New J. Chem.*, 1992, **16**, 855.
49 D. A. Buckingham, A. M. Sargeson and F. P. Dwyer, *Aust. J. Chem.*, 1964, **17**, 622.
50 K. D. Demadis, E. S. El-Samanody, T. J. Meyer and P. S. White, *Polyhedron*, 1999, **18**, 1587.
51 T. L. J. Huang and D. J. Brewer, *Can. J. Chem.*, 1981, **59**, 1689.
52 K. T. Potts and P. A. Winslow, *J. Org. Chem.*, 1985, **50**, 5405.
53 S. A. Savage, A. P. Smith and C. L. Fraser, *J. Org. Chem.*, 1998, **63**, 10048.
54 B. M. Kellybasetti, I. Krodkiewska, W. H. F. Sasse, G. P. Savage and G. W. Simpson, *Tetrahedron Lett.*, 1995, **36**, 327.
55 B. Imperiali, T. J. Prins and S. L. Fisher, *J. Org. Chem.*, 1993, **58**, 1613.
56 H. Brederec, G. Simchen and R. Wahl, *Chem. Ber./Recl.*, 1968, **101**, 4048.
57 M. G. Vetelino and J. W. Coe, *Tetrahedron Lett.*, 1994, **35**, 219.
58 P. Dupau, T. Renouard and H. LeBozec, *Tetrahedron Lett.*, 1996, **37**, 7503.
59 G. Denti, S. Serroni, S. Campagna, A. Juris, M. Ciano and V. Balzani, in *Perspectives in Coordination Chemistry*, ed. A. F. Williams, C. Floriani and A. E. Merbach, VHCA and VCH, Basel and Weinheim, 1992, pp. 153–164.
60 E. C. Constable, C. E. Housecroft and Y. Tao, to be published.
61 All values listed for the trimeric and dimeric compounds were determined by differential pulse voltammetry (DPV). These values were compared with numbers determined by cyclic voltammetry (CV), but did not differ significantly (<20 mV).
62 For better comparison, the redox potentials of $[Ru(bipy)_3]^{2+}$ and $[Ru(terpy)_2]^{2+}$ for measured under the same conditions and also with Fc/Fc^+ as internal reference. The results are in accordance with the values taken from: A. Juris, V. Balzani, F. Barigelletti, S. Campagna, P. Belser and A. von Zelewsky, *Coord. Chem. Rev.*, 1988, **84**, 85–277.
63 E. C. Constable and A. Thompson, *J. Chem. Soc., Dalton Trans.*, 1994, 1409.
64 C. Creutz and H. Taube, *J. Am. Chem. Soc.*, 1973, **95**, 1086.
65 J. P. Sauvage, J. P. Collin, J. C. Chambron, S. Guillerez, C. Coudret, V. Balzani, F. Barigelletti, L. De Cola and L. Flamigni, *Chem. Rev.*, 1994, **94**, 993.
66 V. Balzani, A. Juris, M. Venturi, S. Campagna and S. Serroni, *Chem. Rev.*, 1996, **96**, 759.
67 The DPV of $[(bipy)_2Ru(\mu\text{-}\mathbf{I})Ru(terpy)]^{4+}$ was dominated by one signal. In order to extract the redox potentials, the peak was fitted by two gaussian curves assuming two one-electron processes lying beneath.
68 P. Ceroni, A. Credi, V. Balzani, S. Campagna, G. S. Hanan, C. R. Arana and J. M. Lehn, *Eur. J. Inorg. Chem.*, 1999, 1409.
69 A. J. Bard and L. R. Forster, *Electrochemical Methods, Fundamentals and Applications*, John Wiley & Sons, New York, 2nd edn., 2001.
70 Two reductions for the terpy were observed, although in Fig. 3(A) – dashed line – only one peak is shown.
71 It should also be mentioned that latest studies indicate that this assumption is not entirely correct for related compounds such as Ru and Os phenolate complexes: T. E. Keyes, D. Leane, R. J. Forster, C. G. Coates, J. J. McGarvey, N. Nieuwenhuyzen, E. Figgemeier and J. G. Vos, *Inorg. Chem.*, 2002, **41**, 5721.
72 E. C. Constable, C. E. Housecroft, E. R. Schofield, S. Encinas, N. Armaroli, F. Barigelletti, L. Flamigni, E. Figgemeier and J. G. Vos, *Chem. Commun.*, 1999, 869.
73 M. Duati, S. Fanni and J. G. Vos, *Inorg. Chem. Commun.*, 2000, **3**, 68.
74 J. R. Winkler, T. L. Netzel, C. Creutz and N. Sutin, *J. Am. Chem. Soc.*, 1987, **109**, 2381.
75 Y. Kim and C. M. Lieber, *Inorg. Chem.*, 1989, **28**, 3990.